Subtropical Forcing of Tropical Pacific Climate and Decadal ENSO Modulation

DANIELA MATEI

Max Planck Institute for Meteorology, and International Max Planck Research School on Earth System Modelling, Hamburg, Germany

NOEL KEENLYSIDE AND MOJIB LATIF

Leibniz-Institute of Marine Sciences at the University of Kiel, Kiel, Germany

JOHANN JUNGCLAUS

Max Planck Institute for Meteorology, Hamburg, Germany

(Manuscript received 4 June 2007, in final form 24 January 2008)

ABSTRACT

The relative impact of the subtropical North and South Pacific Oceans on the tropical Pacific climate mean state and variability is estimated using an ocean–atmosphere–sea ice coupled general circulation model. Tailored experiments are performed in which the model is forced by idealized sea surface temperature anomalies (SSTAs) in the subtropics of both hemispheres. The main results of this study suggest that subtropical South Pacific climate variations play a dominant role in tropical Pacific decadal variability and in the decadal modulation of El Niño–Southern Oscillation (ENSO).

In response to a 2°C warming in the subtropical South Pacific, the equatorial Pacific SST increases by about 0.6°C, approximately 65% larger than the change in the North Pacific experiment. The subtropics affect equatorial SST mainly through atmosphere–mixed layer interactions in the South Pacific experiments; the response is mostly accomplished within a decade. The "oceanic tunnel" dominates in the North Pacific experiments; the response takes at least 100 yr to be accomplished. Similar sensitivity experiments conducted with the stand-alone atmosphere model showed that both air–sea interactions and ocean dynamics are crucial in shaping the tropical climate response.

The statistics of ENSO exhibit significant changes in amplitude and frequency in response to a warming/cooling of the subtropical South Pacific: a 2°C warming (cooling) of subtropical South Pacific SST reduces (increases) the interannual standard deviation by about 30% (20%) and shortens (lengthens) the ENSO period. The simulated changes in the equatorial zonal SST gradient are the main contributor to the modulation of ENSO variability. The simulated intensification (weakening) of the annual cycle in response to an enhanced warming (cooling) in subtropical South Pacific partly explains the shifts in frequency, but may also lead to a weaker (stronger) ENSO. The subtropical North Pacific thermal forcing did not change the statistical properties of ENSO as strongly.

1. Introduction

In addition to the interannual changes, the Pacific region experiences climate fluctuations on decadal and longer time scales. Although the decadal ENSO-like pattern in the tropical Pacific and its relation to the North Pacific decadal variability has been extensively studied in the past decade, using both observations and models (Nitta and Yamada 1989; Trenberth and Hurrell 1994; Zhang et al. 1997; Barnett et al. 1999; Pierce et al. 2000; Deser et al. 2004; D'Arrigo et al. 2005), the physical mechanisms responsible for decadal Pacific climate variability are still controversial (Miller and Schneider 2000). It is not clear, for instance, whether the decadal variability is internal to tropical Pacific, or whether the midlatitudes independently undergo decadal variability (Latif and Barnett 1994) and/or affect ENSO variability.

Corresponding author address: Daniela Matei, Max Planck Institute for Meteorology, and International Max Planck Research School on Earth System Modelling, Bundesstr. 53, D-20146 Hamburg, Germany.
E-mail: daniela.matei@zmaw.de

DOI: 10.1175/2008JCLI2075.1

One of the theories for Pacific decadal variability involves the connection between the subtropics/extratropics and tropics through the ocean [the so-called oceanic tunnel (OT)] and/or atmosphere [the so-called atmospheric bridge (AB)] at decadal time scales. Various hypotheses based on a hierarchy of models have been proposed to explain the subtropical–tropical connections, often with contradicting results.

On the one hand, the mean advection mechanism (Gu and Philander 1997) assumes that the subtropical sea surface temperature (SST) anomalies are first subducted into the thermocline. These are then advected to the equator within the subsurface branch of the subtropical cell (STC; McCreary and Lu 1994), and finally upwelled to the surface in the eastern equatorial Pacific, where they affect the cold tongue SST. Recent studies, however, suggest that the temperature anomalies subducted into the pycnocline in the subtropical North Pacific may not reach the equator with any appreciable amplitude (Schneider et al. 1999a,b; Nonaka and Xie 2000). These anomalies, although important for generating subsurface variability in the subtropical gyre (Deser et al. 1996; Zhang et al. 2001), can either be strongly dissipated, dispersed in the form of planetary-scale oceanic waves, or become obscured by the wind-forced variations at low latitudes (Schneider et al. 1999a,b; Nonaka and Xie 2000).

On the other hand, the subtropical anomalies can induce changes in the overlying atmospheric circulations that could result in changes of the STC strength. In this scenario, the varying amount of cool subtropical thermocline water that eventually upwells in the eastern equatorial ocean can change the tropical climate (perturbation advection mechanism). Using an intermediate complexity coupled model, consisting of a 3.5-layer shallow-water model coupled to a statistical atmospheric model, Kleeman et al. (1999) have shown that decadal variations of tropical SSTs are primarily related to changes in wind stress and subduction rates in the subtropics (poleward of $\sim 23°$). Employing an OGCM forced by observed winds, Nonaka et al. (2002) found that equatorial winds (5°S–5°N) are as important as extraequatorial winds (poleward of 5°) for the decadal modulation of equatorial SSTs. The mechanism of tropical decadal variability proposed by Kleeman et al. (1999) was supported by the observational studies of McPhaden and Zhang (2002, 2004) and the modeling work of Lohmann and Latif (2005). They presented evidence that the warming and cooling events and mass transport anomalies seem to be related over the last 40–50 yr.

The subtropical/midlatitude climate can also affect the tropics through the atmospheric teleconnections. Barnett et al. (1999) argued that anomalous winds related to a midlatitude decadal mode in the North Pacific may extend to the equatorial region, affect the equatorial thermocline and modulate ENSO. Pierce et al. (2000) also found that the strongest link between tropics and midlatitudes on decadal time scales is communicated almost simultaneously via changes in surface wind stress. Recent research has also identified a "seasonal footprinting mechanism" by which midlatitude atmospheric variability can affect the evolution of tropical Pacific interannual variability via coupled interactions in the subtropics (Vimont et al. 2001).

The subtropical Pacific climate variations can produce not only persistent decadal changes in the tropical Pacific, but may also modulate the behavior of ENSO through changes in the background mean state. How ENSO responds to a background state change has recently attracted much attention, particular in relation to global warming (Van Oldenborgh et al. 2005; Zelle et al. 2005; Merryfield 2006; Guilyardi 2006; Meehl et al. 2006b). The current generation of coupled ocean–atmosphere general circulation models predicts substantially different SST patterns in the tropical Pacific when run under anthropogenic climate change scenarios (Collins et al. 2005; Van Oldenborgh et al. 2005). While some of the models show a mean El Niño–like response in the tropical Pacific SST (stronger warming in the east), other models exhibit a stronger warming in central Pacific or even a La Niña–like response (stronger warming in the west). Liu et al. (2005) reexamined the response of tropical Pacific SST to increased atmospheric CO_2 concentration with an emphasis on the latitudinal SST gradient, instead of the traditionally studied zonal SST gradient. They argued that the enhanced equatorial warming (EEW) relative to the subtropics is a more robust tropical SST fingerprint of global warming (see Fig. 3 in their paper). It is not clear how this different SST response of subtropical and tropical Pacific to greenhouse warming may affect ENSO characteristics.

In the last decade, the potential influence of North Pacific ocean–atmosphere processes on tropical Pacific decadal variability has dominated the literature, probably also due to the sparse observational data over the Southern Ocean. More recently, a number of observational (Wang and Liu 2000; Luo and Yamagata 2001; Giese et al. 2002; Holland et al. 2006) and numerical modeling studies (Luo et al. 2003, 2005) have shown pronounced subsurface signals moving from South Pacific to the equatorial region. Hence, an important question to be addressed is: what are the relative roles of the subtropical North and South Pacific in the decadal modulation of tropical SSTs?

Because of insufficient observational data for these time scales, coupled models are essential tools for identifying the physics responsible for decadal variability in the climate system. Although previous research on extratropical–tropical interactions has been carried out separately either in an atmosphere model or in an ocean model, the full climate impact of these teleconnections can only be assessed from the coupled perspective. In a recent coupled GCM study (Liu and Yang 2003), the extratropical impact on tropical climate is quantified using the so-called partial coupling experiments. In this experiment, a 2°C SST anomaly is "seen" by both the atmosphere and ocean in the global extratropics ($>|30°|$ latitude) and is then "carried" equatorward by both the atmospheric bridge and the oceanic tunnel. The atmosphere and ocean remain fully coupled only within the global tropics ($<|30°|$ latitude). This extratropical warming is found to increase the remote equatorial ocean temperature by ~1°C in the surface and subsurface, with the dominant influence on the equatorial climate coming from the Southern Hemisphere. Further analyses and experiments indicate that, while the SST change is mainly caused by the atmospheric bridge involving changes in the Hadley circulation, the subsurface temperature change is accomplished predominantely through the oceanic tunnel. Using similar idealized experiments, Yang et al. (2005b) showed that the remote impact of the extratropics on the tropics can modulate ENSO behavior. An extratropical climate warming leads to a weaker Hadley circulation in both hemispheres and a slow down of the mean shallow meridional overturning circulation in the upper Pacific. This causes a reduction in the equatorward cold water supply and equator upwelling and therefore, a weakened stratification of the equatorial thermocline. This leads to a weaker and longer ENSO cycle.

In this study, we employ a state-of-art ocean–atmosphere coupled model to investigate how the changes in the subtropical Pacific climate mean state may affect the mean tropical Pacific climate and ENSO variability. Here we use localized SST forcing over subtropical Pacific, as opposed to a basinwide SST anomaly in Liu and Yang (2003). This approach is not only more realistic for the study of climate variability, but also clearer in illustrating the mechanisms of the equatorward teleconnection. The paper is organized as follows: In section 2, we introduce the coupled model and the experimental setup of the sensitivity experiments. Section 3 is focused on the impact of subtropical thermal variations on the mean state of tropical Pacific Ocean, while the modulation of ENSO variability by the subtropical Pacific thermal forcing is explored in section 4. Conclusions are provided in section 5.

2. Model and experimental setup

The coupled atmosphere–ocean–sea ice model used in this study is the state-of-the-art coupled general circulation model ECHAM5/Max Planck Institute Ocean Model (MPI-OM) developed at the Max Planck Institute for Meteorology (MPI). A detailed description of the atmosphere GCM ECHAM5 can be found in Roeckner et al. (2003) and in the special issue of the *Journal of Climate* (2006, Vol. 19, No. 16) on the ECHAM5/MPI-OM model (Roeckner et al. 2006). The ECHAM5 version we employ here is the "tropospheric model," resolving the atmosphere up to the middle stratosphere (10 hPa). It has 19 irregularly distributed vertical levels, with the highest vertical resolution in the atmospheric boundary level. The horizontal spectral resolution is T31, corresponding to approximately 3.75°. The ocean model, MPI-OM (Marsland et al. 2003), is a version of the Hamburg Ocean Primitive Equation (HOPE) model using a C-grid and orthogonal curvilinear coordinates. The model includes a Hibler-type dynamic/thermodynamic sea ice model and a river runoff scheme. The ocean grid is similar to the one described in Jungclaus et al. (2006), but with coarser resolution. The horizontal resolution of this model version is about 3° on average and varies from a minimum of 20 km in the Arctic to a maximum of about 350 km in the tropics. The coupled model does not employ flux adjustment or any other corrections.

The 1000-yr-long control integration of the coupled model exhibits a stable climate. The mean climatological state of the tropical Pacific is shown in Fig. 1. The dominant simulated tropical Pacific interannual signal has a spatial pattern that is broadly similar to the observed one. Nevertheless, there are several differences between the modeled and the observed ENSO. First, the simulated ENSO variability is stronger than observed. Second, the modeled ENSO pattern is more equatorially confined and extends too far westward compared to observations. The coupled model has a realistic ENSO period with maximum variance at a period of about 3 yr. However, in contrast to the observed broad spectral peak between 2 and 7 yr, the model spectral peak is too sharp, indicating far too regular variability. The ENSO dynamics seem to be similar to that of the observations, with slow eastward-propagating equatorial heat content anomalies and a standing SST pattern (not shown). The above-mentioned differences between the model and observed tropical Pacific interannual variability represent

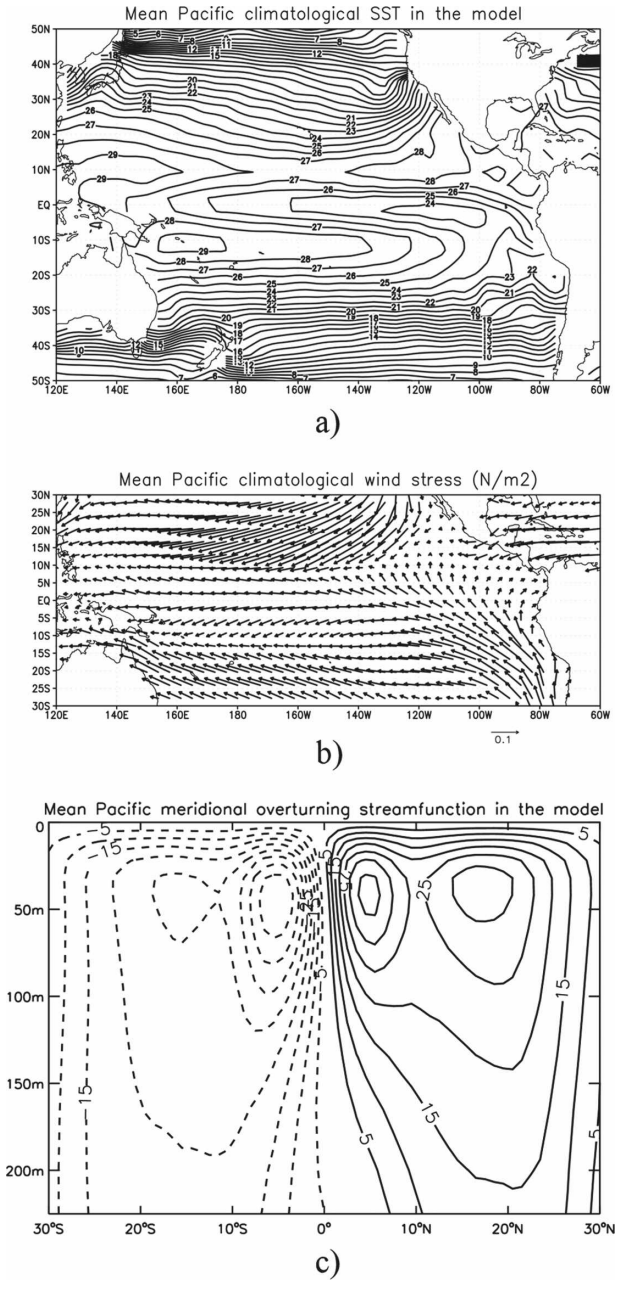

FIG. 1. Climatogical state of the tropical Pacific in the ECHAM5/MPI-OM model: (a) mean sea surface temperature (°C), (b) mean wind stress (N m^{-2}), (c) mean Pacific meridional overturning streamfunction (Sv; 1 Sv = 10^6 m^3 s^{-1}). The contour interval in (a) is 1°C. The reference vector in (b) is 0.1 N m^{-2}. The contour interval in (c) is 5 Sv. Solid (dashed) lines represent clockwise (anticlockwise) flow.

typical systematic errors of coupled models (Latif et al. 2001). Like many other coupled models, ECHAM5/MPI-OM suffers from an equatorial cold bias and a too westward extension of the equatorial cold tongue (Fig. 1a).

Here our primary interest is in the subtropical modulation of the tropical Pacific mean climate and ENSO variability. To investigate the climate response of the equatorial Pacific system to thermal variations in the subtropical surface climate, and to estimate the relative contributions of the North and South Pacific to the subtropical–tropical connections, we carried out a number of partial coupling experiments. In these sensitivity experiments, the coupled model is forced by idealized SST anomalies either over the North Pacific or South Pacific subtropics. Two domains were selected, one in the subtropical North Pacific (hereafter NPac) between 23°–31°N and 170°–125°W, and the second one in the subtropical South Pacific (hereafter SPac) between 23°–31°S and 135°–75°W. The two selected domains (Fig. 2) are in the regions of subduction windows (Liu et al. 1994; Gu and Philander 1997; Huang and Liu 1999). In selecting the size of the forcing domains, the relative coarse horizontal resolution of the coupled model was also taken into consideration. We have imposed a homogenous 2° warming/cooling on the top of the mean seasonal cycle of the control run over the NPac and SPac domains. The SST forcing was applied in the uppermost layer of the ocean. Outside the selected domains we allowed full ocean–atmosphere coupling. The SST anomalies were kept constant for 200 yr. The prescribed 2°C anomaly is beyond the range of intrinsic coupled variability, but is within the range of the expected global warming change in the subtropical Pacific in the model (not shown) and literature (Kerr 2004; Lea 2004).

Negative (−2°C) SST sensitivity experiments were performed in order to study the equatorial response to an idealized cooling in the subtropical Pacific. To further assess the linearity of the equatorial response, we have also conducted experiments with half of the forcing: +1°C/−1°C. Additionally, SSTA integrations with the stand-alone atmospheric model are performed to identify the combined role of ocean dynamics and ocean–atmospheric coupling in subtropical–tropical interactions. In the following, the response of a coupled experiment is computed as the difference between the mean of a variable over the whole 200 yr of the experiment and the mean of the control run for the same period. Only the response that exceeds the 95% significance level according to a two-sided Student's *t* test is discussed.

3. Subtropical impact on tropical Pacific mean climate

We first explore the adjustment of the tropical Pacific to an enhanced warming in the subtropical South Pa-

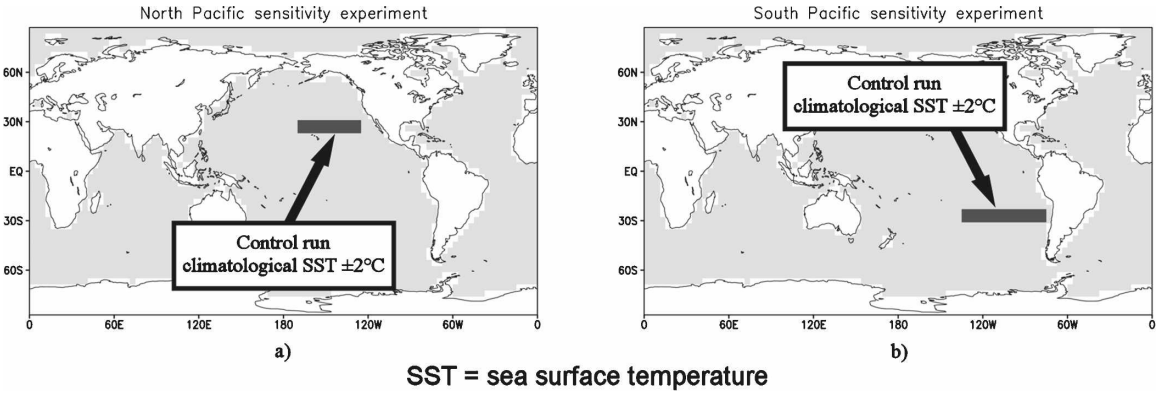

FIG. 2. Selected domains of the individual sensitivity experiments: (a) North Pacific experiment (NPac) and (b) South Pacific experiment (SPac).

cific (SPac+2°C) and North Pacific (NPac+2°C), respectively, in order to quantify the relative impact of the subtropical North and South Pacific on the tropical climate. The impact of subtropical warming versus subtropical cooling is also discussed.

The equatorial Pacific SST change, computed as the sea surface temperature response averaged between 5°S–5°N and 120°E–80°W, is +0.58°C in the SPac+2°C experiment, compared to +0.35°C in the NPac+2°C (i.e., about 65% larger for the South Pacific experiment). The magnitude of the tropical warming here is comparable with that of Yang and Liu (2005) for the case of single hemispheric forcing. In their study, after 200 yr of simulation, the final tropical SST change in response to a 2°C Southern Hemisphere (Northern Hemisphere) forcing is about 0.67°C (0.5°C). This can be explained by the fact that although the anomaly domain in our experiments is smaller than the basinwide anomaly in Yang and Liu, it is however located predominantly in the subduction exchange window. It is also located in a key atmospheric region with respect to the trade winds. Therefore, it may capture almost all the subduction signal of a basinwide anomaly case. A similar difference in the impact of subtropical North and South Pacific forcing is simulated for the cooling experiments: a 2°C cooling in the subtropical South Pacific causes a 0.62°C cooling of the equatorial Pacific SST compared to only 0.35°C in the subtropical North Pacific (not shown). Furthermore, the thermal forcing of the subtropical South Pacific has a maximum impact on the eastern tropical Pacific climate, while the impact of the subtropical North Pacific is mostly confined to the western tropical Pacific (cf. Figs. 3c and 3f). The subtropical North and South Pacific Oceans also have a different impact on the equatorial thermocline structure (cf. Figs. 4c and 4f).

We shall now explain the different impacts of North and South Pacific, limiting the discussion to the warming experiments (NPac+2°C and SPac+2°C). After only 10 yr of simulation, the equatorial response in the SPac+2°C experiment is almost fully developed (cf. Figs. 3d and Figs. 3e,f). This relatively rapid increase in the equatorial SST suggests a dominant role of atmosphere–mixed layer interactions in the remote impact of the subtropical South Pacific. Anomalous northwesterly trades (Fig. 5c) that reduce the evaporative heat loss in the eastern tropical South Pacific, accompany the enhanced warming in the subtropical South Pacific. In this way the subtropical South Pacific warming extends farther into the eastern tropics. The pattern is indicative of the coupled wind–evaporative–SST (WES) feedback between the atmosphere boundary layer and ocean (Xie and Philander 1994) that was shown to produce a rapid equatorward and westward propagation of extratropical SST disturbances by Liu and Xie (1994) and Liu (1996). After reaching the equator, the SST anomalies are further intensified by the local coupled ocean–atmosphere (Bjerknes) feedback. The WES feedback not only leads to a very fast change of equatorial SST, but also forces a spindown of the meridional overturning circulation in the upper Pacific (Fig. 6b). This reduction in upwelling further amplifies the tropical SST change.

In the first years of the SPac+2°C simulation, the dynamical adjustment of the equatorial thermocline to the zonal wind stress changes leads to a surface warming and a cooling at depth (Fig. 4d). This is followed by a slow warming from below as the experiment continues (Fig. 4e,f), which suggests that "ocean tunnel" also plays a role in the South Pacific subtropical–tropical connections at the multidecadal time scale. This is further supported by the steady increase in the equatorial Pacific heat content at 0.35°C $(200\ \text{yr})^{-1}$ (Fig. 7).

The equatorial climate change in response to sub-

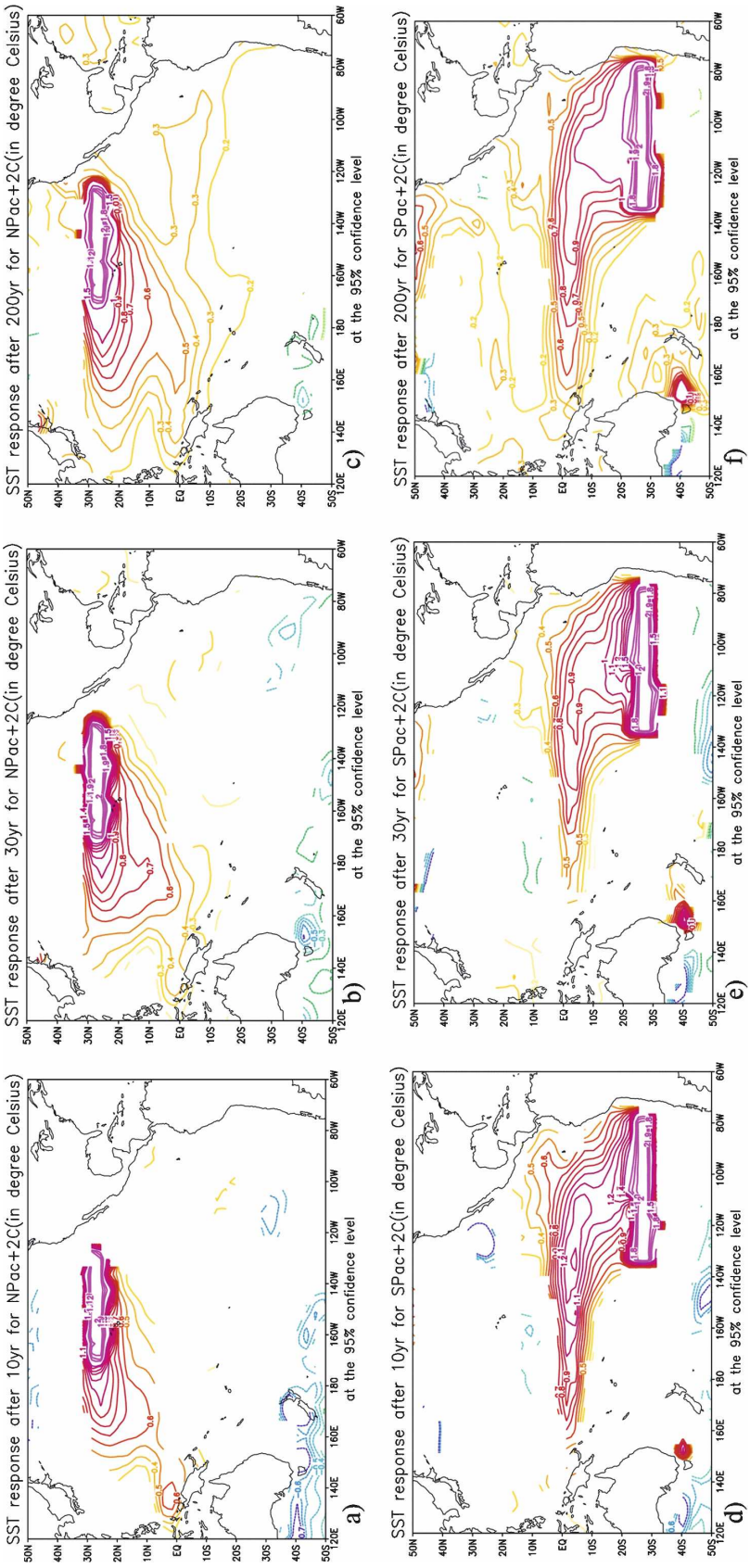

FIG. 3. Anomalous Pacific Ocean SST (°C) after the first (a), (d) 10, (b), (e) 30, and (c), (f) 200 yr in the (a)–(c) NPac+2°C and (d)–(f) SPac+2°C experiments. The contour interval is 0.1°C. Please note that values in the range (−0.2°C, +0.2°C) are not plotted. Response is the difference computed over the indicated periods from the mean of the 200-yr control.

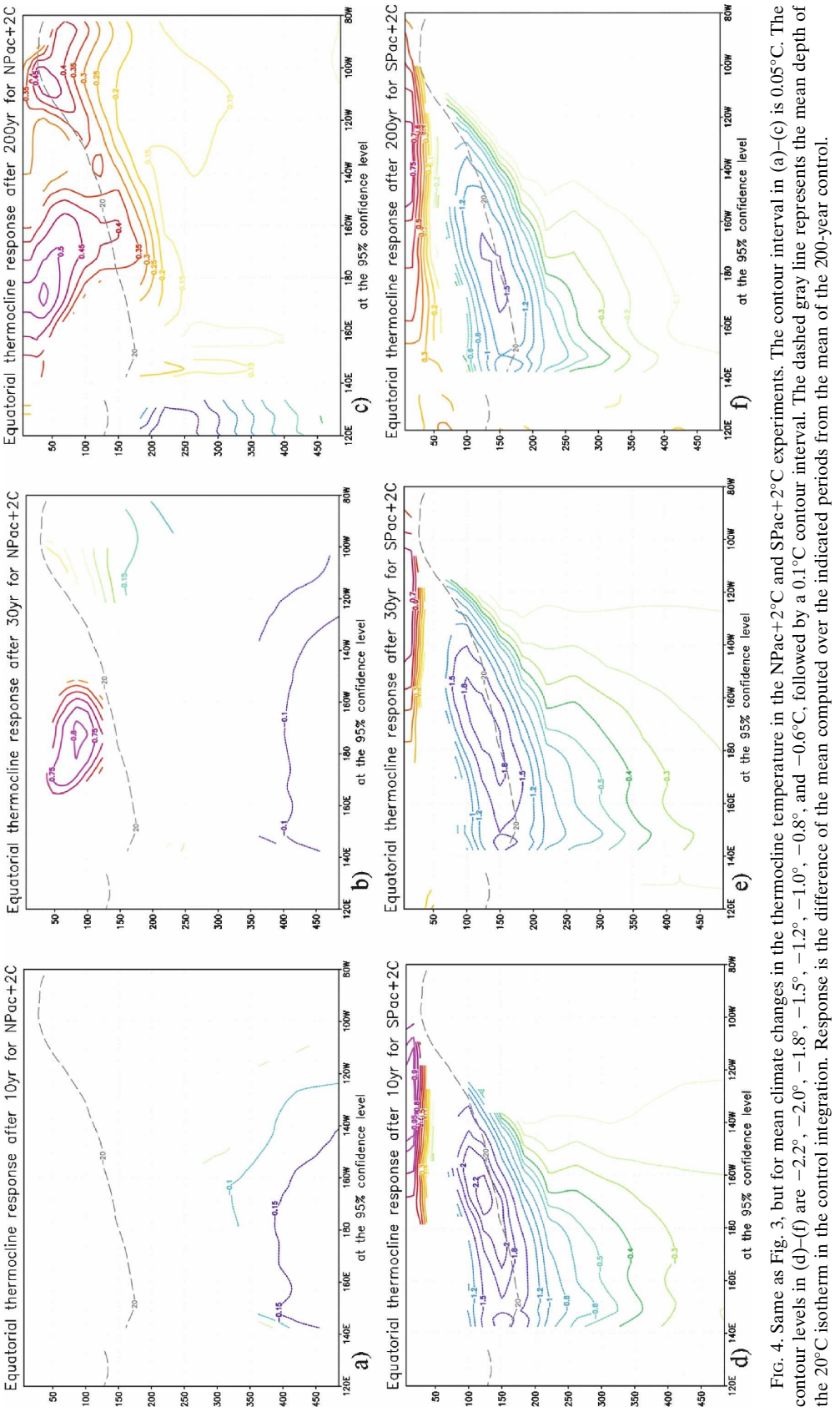

FIG. 4. Same as Fig. 3, but for mean climate changes in the thermocline temperature in the NPac+2°C and SPac+2°C experiments. The contour interval in (a)–(c) is 0.05°C. The contour levels in (d)–(f) are −2.2°, −2.0°, −1.8°, −1.5°, −1.2°, −1.0°, −0.8°, and −0.6°C, followed by a 0.1°C contour interval. The dashed gray line represents the mean depth of the 20°C isotherm in the control integration. Response is the difference of the mean computed over the indicated periods from the mean of the 200-year control.

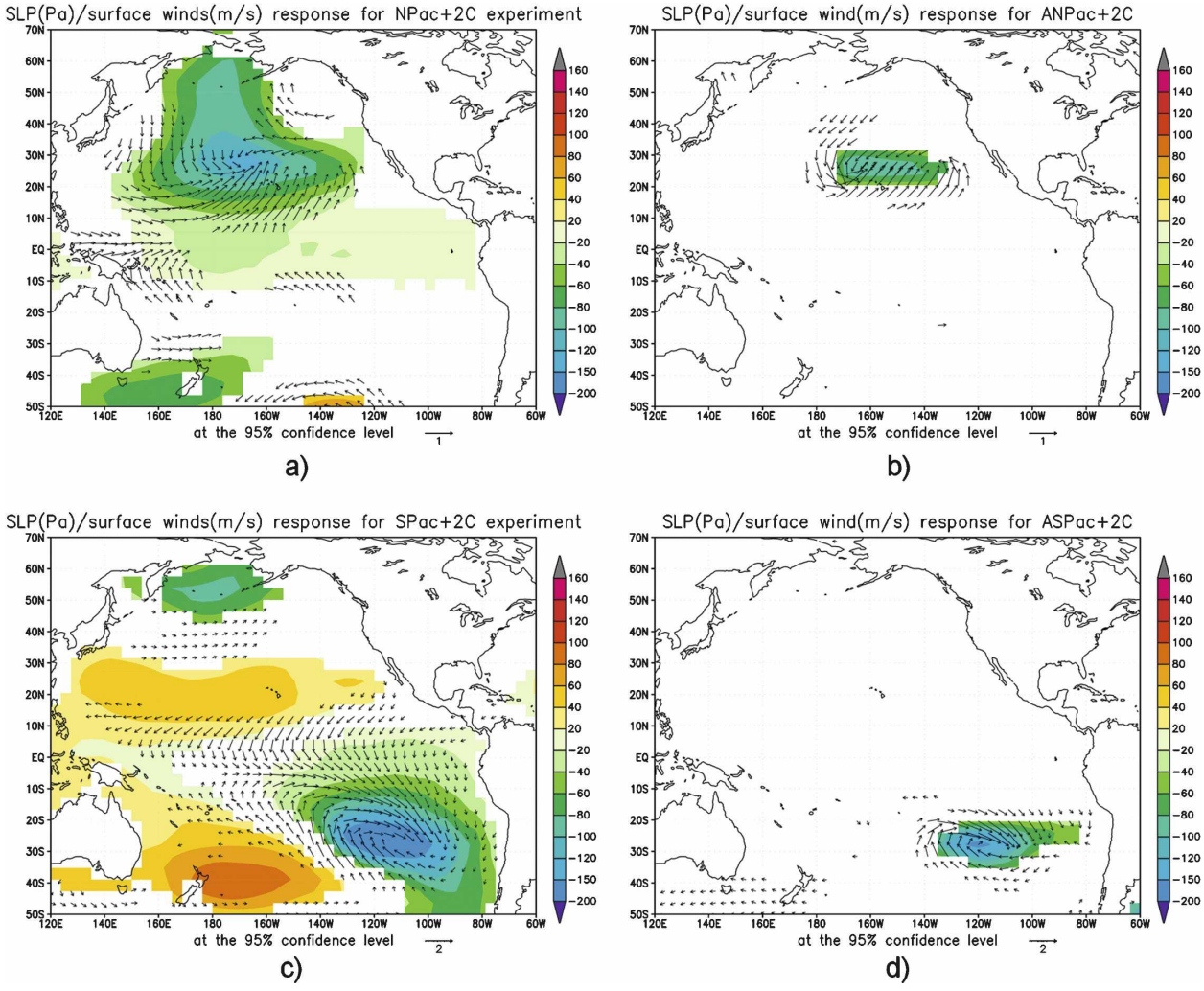

FIG. 5. Anomalous Pacific Ocean sea level pressure (Pa) and surface wind speed (m s^{-1}) in the (a) NPac+2°C, (b) ANPac+2°C, (c) SPac+2°C, and (d) ASPac+2°C experiments. The reference vector in (a), (b) is 1 m s^{-1} and in (c), (d) is 2 m s^{-1}.

tropical North Pacific warming is confined to the westernmost part of the warm pool region during the first 10 yr of the experiment (Fig. 3a), and is accompanied by no significant mean changes in the subsurface temperature (Fig. 4a). The fast increase in SST over the west tropical Pacific can also be attributed to the WES coupled feedback. The cyclonic response in sea level pressure in the tropical North Pacific (Fig. 5a) is associated with anomalous southwestern trades that will warm the SST through a reduction in evaporation. The propagation of these positive SST anomalies toward the warm pool region is accompanied by westerly wind anomalies that will further reduce the evaporative heat loss and warm the sea surface (Fig. 5a). Our results are in accordance with a recent study of Wu et al. (2006). Using both observations and a coupled ocean–atmosphere model, they proposed the WES feedback as a possible mechanism for the extratropical–tropical connections in the North Pacific, and suggested that the recent tropical Pacific decadal climate variability originates from the extratropical North Pacific.

While the same relatively fast atmosphere–mixed layer interactions seem to act in both the North and South Pacific experiments, the amplitude and the spatial extension of the response are very different. Even after 30 yr of simulation, the SST warming in the NPac+2°C experiment is limited to the western tropical Pacific between 120°E and 180°, reaching a maximum of only 0.5°C (Fig. 3b). At the same time, a 0.8°C warming appears in the upper equatorial ocean between 50 and 150 m and tends to propagate eastward along the thermocline (Figs. 4b,c). This SST warming from below

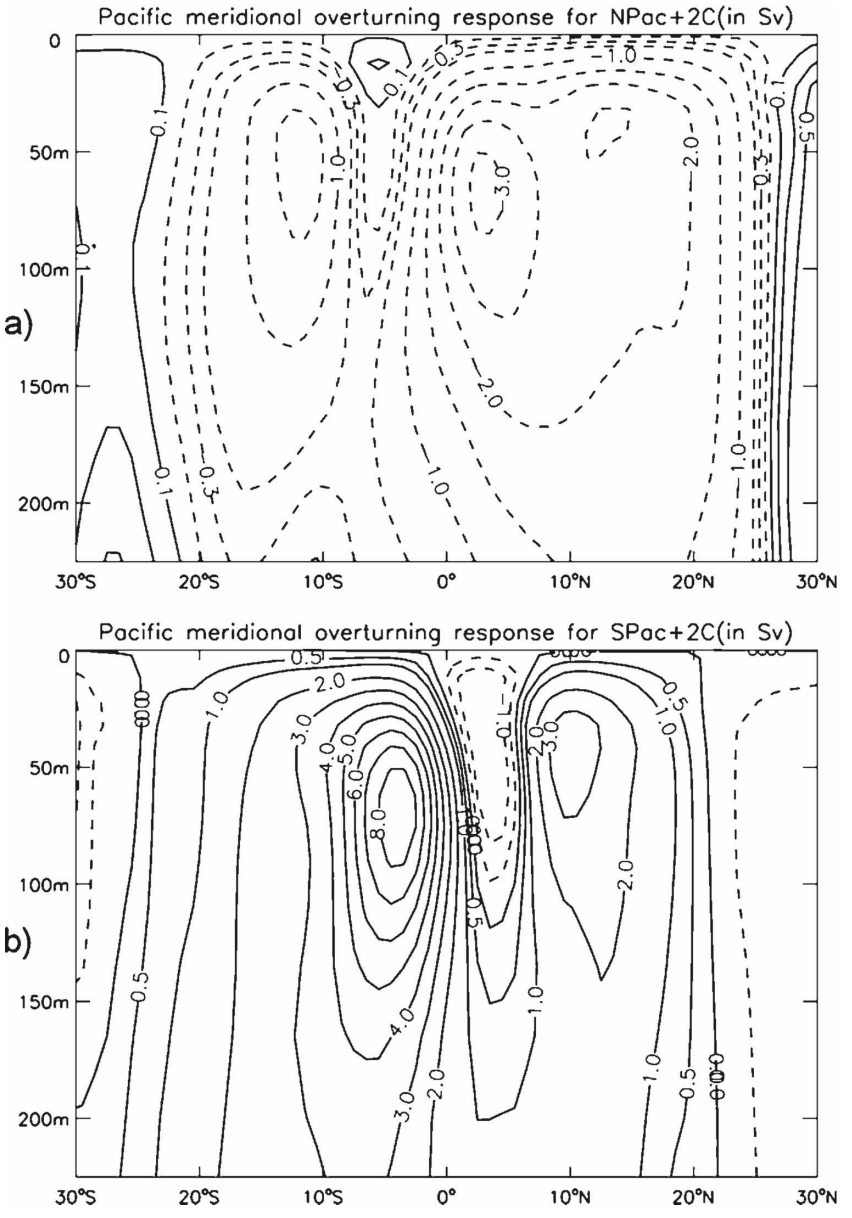

FIG. 6. Anomalous Pacific Ocean meridional overturning streamfunction (Sv) in the (a) NPac+2°C and (b) SPac+2°C experiments. Contour levels in (a) are −3, −2.5, −2, −1.5, −1, −0.5, −0.3, −0.1, 0.1, 0.3, and 0.5 Sv, while contour levels in (b) are −1, −0.5, 0, 0.5, 1, 2, 3, 4, 5, 6, 7, and 8 Sv. Solid (dashed) lines represent clockwise (anticlockwise) flow.

suggests a more important role for the "ocean tunnel" compared to the atmosphere–mixed layer interactions in the NPac+2°C experiment. Since changes in shallow meridional overturning circulation are not large in the NPac+2°C experiment (cf. Figs. 6a and 6b), due to the quite small changes in the equatorial zonal wind stress (not shown), the dominant mechanism in OT remains the isopycnal transport of anomalous temperature signal.

A first-order linear response is simulated for full (±2 K) and half-forcing (±1 K) sea surface temperature sensitivity experiments in both the North and South Pacific. Although the tropical Pacific climate response to an enhanced surface warming/cooling in the subtropics is to first-order linear, the negative thermal forcing has a stronger impact on equatorial Pacific thermocline (not shown). A bigger change in the vertical mixing may explain the larger subsurface temperature

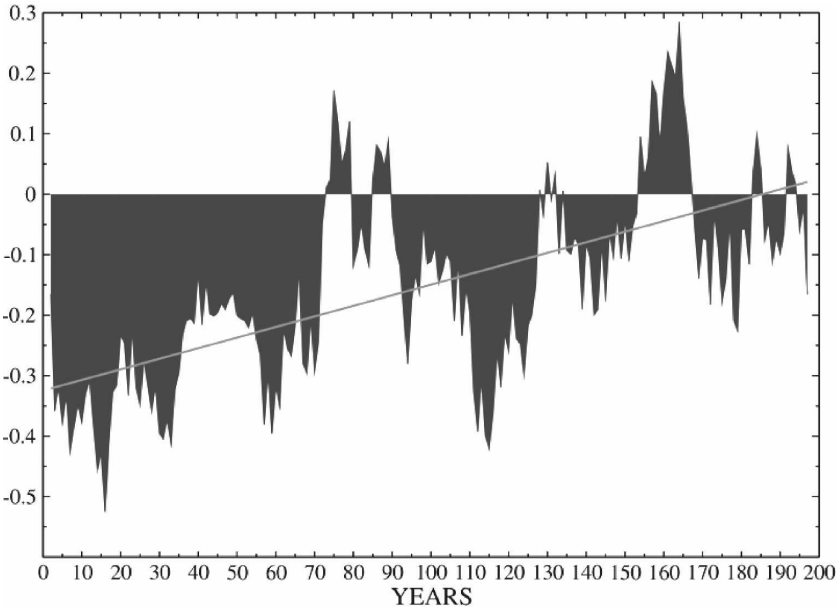

FIG. 7. Time evolution of the equatorial Pacific annual heat content anomaly (°C) averaged over 5°N–5°S, 140°E–80°W in the SPac+2°C experiment. The vertically averaged ocean temperature over the upper 450 m is used as a proxy of the ocean heat content. To highlight the low-frequency variability, a 5-yr running mean is applied to the index.

anomaly in the cold experiments compared to the warm experiments.

To further quantify the role of air–sea interactions and ocean dynamics in the simulated tropical climate response to the subtropical surface warming/cooling, we performed sensitivity experiments, similar to the coupled ones, with the AGCM ECHAM5 only. The sea surface temperature and sea ice monthly climatology for these experiments are taken from the coupled control run. The uncoupled integration has a length of 36 yr and will constitute our AGCM control run (ACTR). After allowing a 6-yr spinup period, we imposed a +2°C SST anomaly over the North Pacific (hereafter ANPac+2°C) and South Pacific domains (hereafter ASPac+2°C) separately, and run two 30-yr-long simulations. All the mean climate changes are derived as the difference between the mean of each AGCM experiment and the mean of control run, ACTR, over the whole (30 yr) period of the sensitivity run. Again, only statistically significant changes at the 95% level according to a two-sided Student's t test are discussed here.

Figure 5d displays the mean sea level pressure change for the ASPac+2°C experiment. In contrast to the coupled experiment, the atmospheric response in the AGCM simulation to the warming in the subtropical South Pacific is mostly confined to the Southern Hemisphere and there is no response in the equatorial Pacific. Correspondingly, the change in the surface wind displays a cyclonic anomalous circulation that is limited to the eastern subtropical South Pacific. Comparing with the South Pacific experiment, the atmospheric response to the subtropical warming in the North Pacific is much weaker (cf. Figs. 5b and 5d). Similar to ASPac+2°C experiment, significant changes in the surface wind are restricted to the forcing region, but they are only about half as strong (cf. Figs. 5b and 5d). The weaker atmospheric response to the thermal forcing in subtropical North Pacific might also contribute to the smaller impact of the North Pacific Ocean on the tropical climate. The considerable difference in the magnitude of the atmospheric response to the subtropical North and South Pacific SST forcing can be attributed to the different latent heat release in the two experiments as inferred from the precipitation response. We can conclude that air–sea interactions and ocean dynamics are very important for the equatorial Pacific response to SST anomalies in the subtropical Pacific.

4. Subtropical impact on tropical Pacific interannual climate variability

The changes in the background tropical climate in our sensitivity simulations have a significant impact on tropical Pacific interannual variability. Here, the changes in variability are first presented, and then the

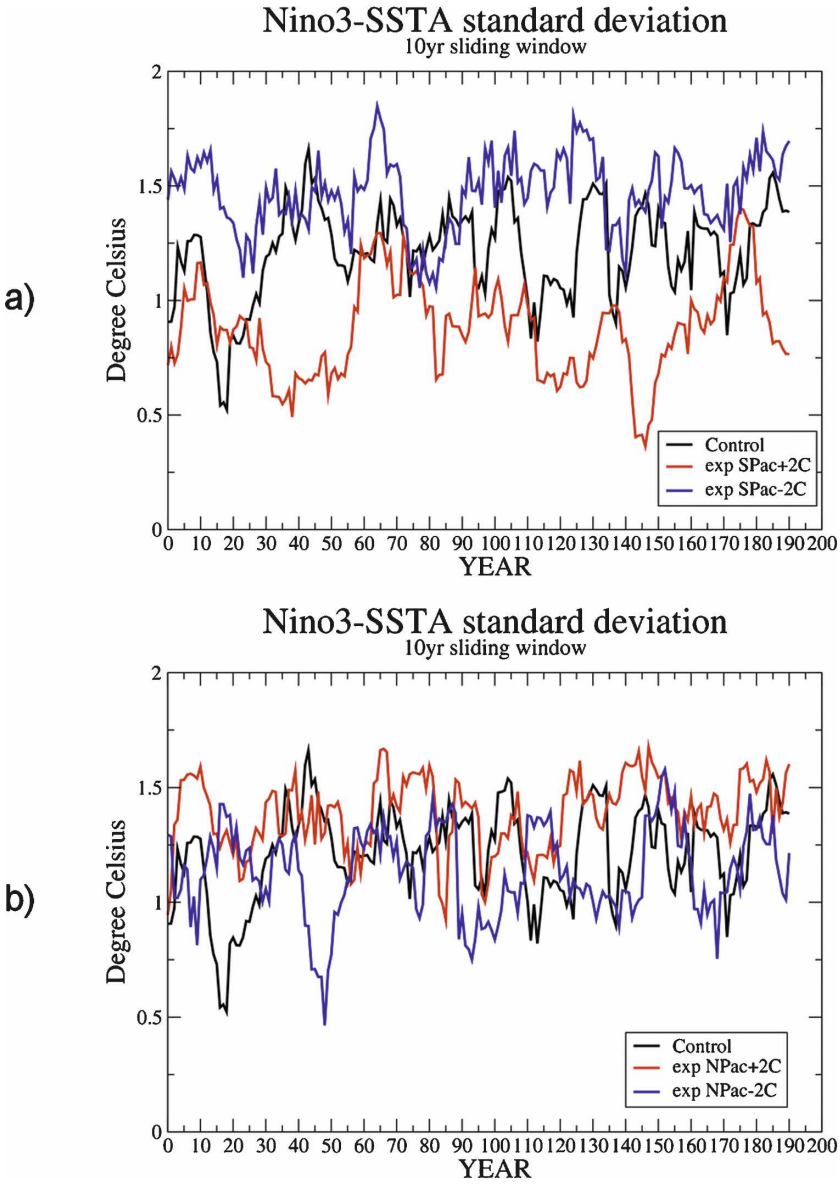

FIG. 8. Standard deviation of Niño-3 SSTA (°C) as a function of time in the (a) Spac±2°C and (b) Npac±2°C experiments. A low-pass filter in the form of a sliding window 10 yr wide was used to compute the standard deviations. Also shown here is the Niño-3 SSTA standard deviation in the control integration (black curve). In both panels, the red curve (blue curve) represents the warming (cooling) experiment in the respective hemisphere.

responsible changes in the mean state, feedbacks, and the annual cycle are described.

a. Simulated changes in ENSO

The statistics of ENSO exhibit extensive changes in amplitude and frequency in response to subtropical South Pacific warming (cooling). Figure 8 shows the standard deviation of the Niño-3 SST anomaly, computed using a 10-yr sliding window, for the SPac±2°C and NPac±2°C experiments. A 2°C subtropical South Pacific SST warming reduces the mean ENSO standard deviation by 28%, while a 2°C subtropical South Pacific SST cooling increases the mean ENSO standard deviation by 21%. A similar change in ENSO intensity occurred in the work of Yang et al. (2005b). They reported a 20% reduction in ENSO amplitude by an enhanced global extratropical warming that is consistent with the results of our SPac+2°C experiment. The sub-

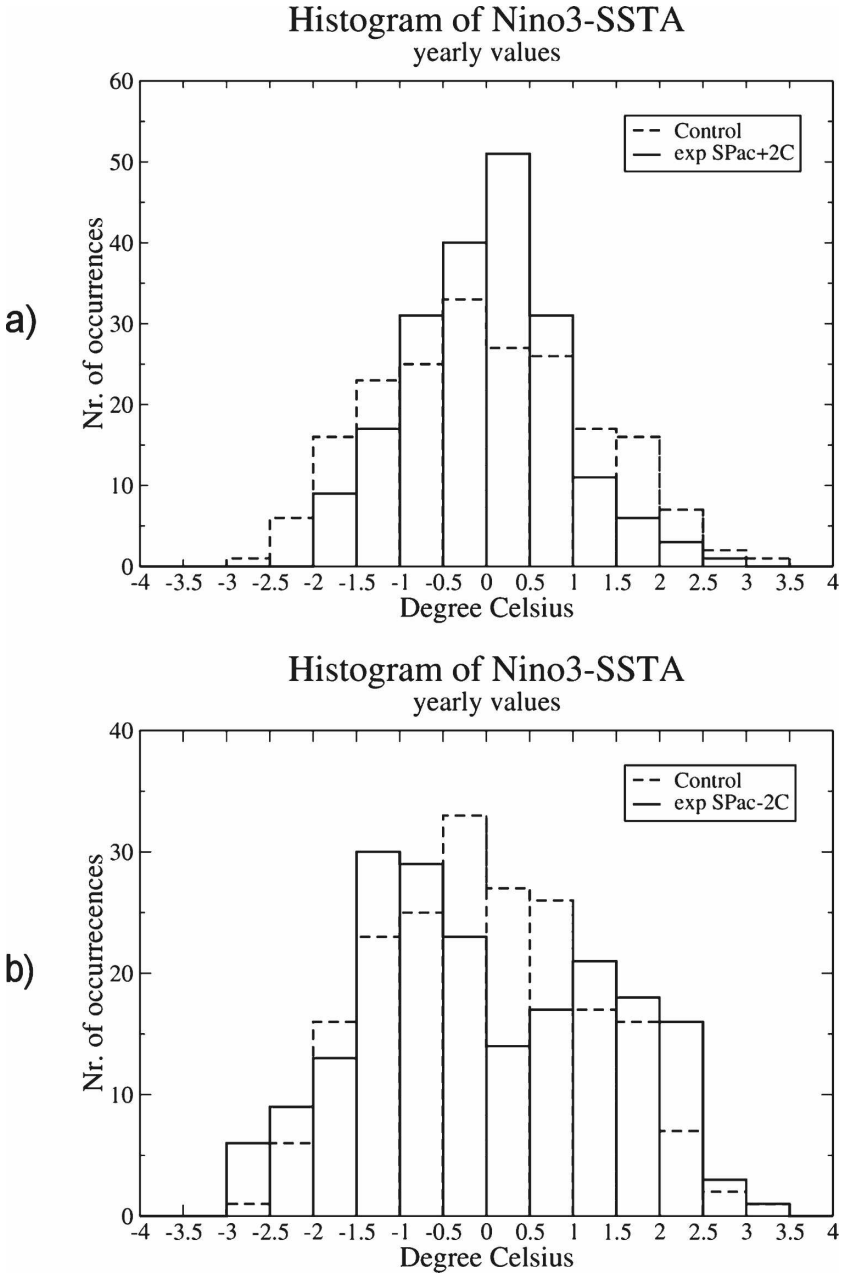

FIG. 9. Frequency distribution of annual Niño-3-SSTA during the (a) SPac+2°C (solid line) and (b) SPac-2°C (solid line) experiments. For comparison, we also show the frequency distribution of annual Niño-3 SSTA during the control integration (dashed line).

tropical North Pacific has an opposite effect on ENSO compared to the subtropical South Pacific: the subtropical North Pacific warming increases ENSO strength by 14%, while the subtropical cooling decreases ENSO strength by 6%. In the following, we shall focus on the ENSO variability changes in the South Pacific sensitivity experiments only, because the impact of subtropical North Pacific on ENSO variability is much smaller in our model.

To further investigate the changes in ENSO statistics, we calculated the frequency distribution of annual Niño-3 SST anomalies. Figures 9a and 9b display the frequency distribution for the SPac+2°C (solid line) and SPac−2°C (solid line) experiments, respectively.

The control run frequency distribution is plotted with a dashed line in both histograms. The distribution obtained from the warming experiment in the South Pacific is narrower than that obtained from the control run, in accordance with the decrease in interannual variability. For the SPac+2°C experiment, the occurrence of weak ENSO extremes increases and the occurrence of strong ENSO extremes decreases. The opposite behavior is simulated in the cooling experiment in the South Pacific, confirming the increased interannual variability, with less frequent weaker ENSO extremes and more frequent, stronger ENSO extremes. In both South Pacific sensitivity experiments and in the control simulation, the distribution of Niño-3 SST anomalies is almost symmetric, indicating no change in the skewness of ENSO. This is confirmed by the estimated skewness of Niño-3 SST anomalies: 0.0623 in the control simulation compared to 0.0664 (0.0033) in the SPac+2°C (SPac−2°C) experiment. The significantly decreased (increased) ENSO variability is also evident in the power spectra of monthly Niño-3 SST anomalies associated with the subtropical South Pacific warming (cooling) (Fig. 10).

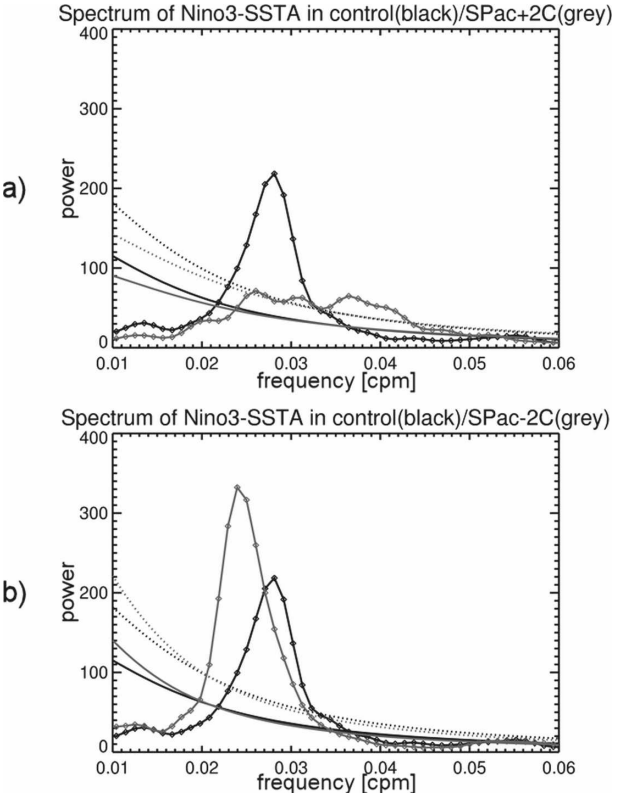

FIG. 10. Power spectra of the simulated Niño-3 SSTA in the (a) SPac+2°C (gray line with diamonds) and (b) SPac−2°C experiments (gray line with diamonds). For comparison, the power spectra of Niño-3 SSTA in the control integration is shown in black. The 95% confidence level is plotted as the dotted line, and the AR1 process fitted to the data as thin solid line.

b. Background state changes

How mean state changes may have lead to changes in the statistics of interannual variability in the South Pacific sensitivity experiments is now discussed. Figure 11 shows the changes in the equatorial zonal SST gradient in the South Pacific experiments. In response to an enhanced warming (cooling), the zonal SST contrast has decreased (increased) by 0.55°C (0.4°C). This influences the zonal advection feedback discussed in the next section. A decrease in the zonal SST contrast favors a reduction in ENSO variability. Our findings are in accordance with those of Merryfield (2006) and Knutson et al. (1997), who found a decrease in ENSO variability under global warming conditions resulting from a reduced zonal SST gradient. This is also supported by the recent study of Sun et al. (2004), who used a simplified ocean–atmosphere coupled model to study the effect of an enhanced subtropical surface cooling on ENSO. Their results suggest that an enhanced cooling in the subtropics results in a regime with stronger ENSO. Through the "ocean tunnel" (Gu and Philander 1997), the stronger subtropical cooling decreases the temperature of the water feeding the Equatorial Undercurrent and therefore, results in colder upwelled water in the eastern equatorial Pacific. The subsequent SST cooling in the eastern equatorial Pacific strengthens the equatorial zonal SST contrast, triggering a regime with stronger ENSO. In our SPac−2°C experiment, the change in the tropical wind spins up the meridional overturning circulation in the upper Pacific. The spinup of the STC in the South Pacific and the TC cells in both hemispheres will increase the amount of water that is upwelled in the eastern equatorial Pacific (Kleeman et al. 1999), resulting in an increased zonal SST contrast and, therefore, a stronger ENSO variability.

Changes in the mean equatorial trade winds can also produce changes in the equatorial thermocline structure that may also alter interannual variability. Figures 12a and 12b display the zonal wind stress and the thermocline depth anomalies associated with the SPac±2°C experiments, which are spatially averaged between 5°S and 5°N. The slackening (intensification) of the equatorial trade winds in response to the warming (cooling) in subtropical Pacific goes along with a shoaling (deepening) of the mean thermocline. The thermocline changes are mostly confined to the western and central equatorial Pacific. According to the idealized modeling study of Fedorov and Philander (2001), an increase in the mean depth of the equatorial thermocline stabilizes

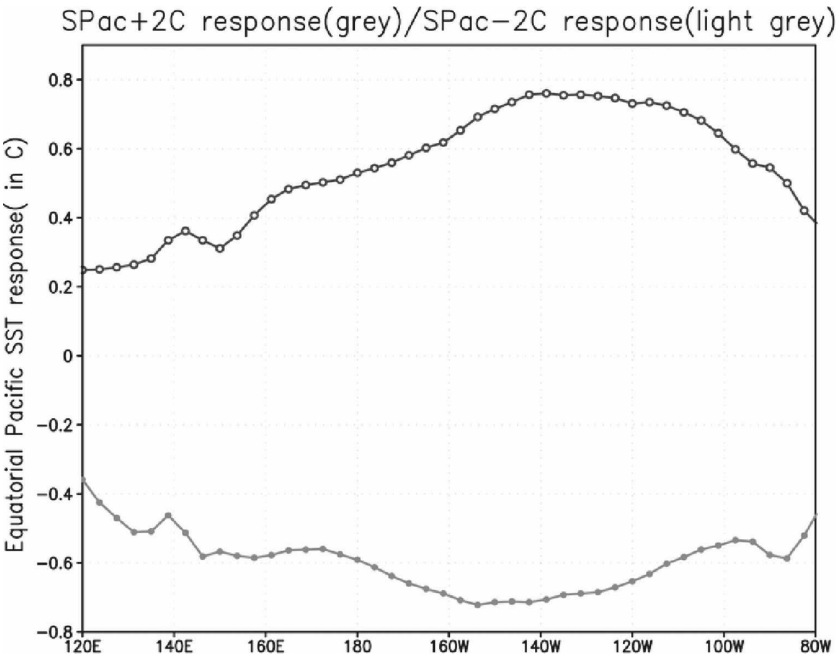

FIG. 11. Anomalous sea surface temperature (°C) in the SPac+2°C (gray curve with open circles) and the SPac−2°C experiments (light gray curve). The anomalies are computed as the spatial average between 5°S and 5°N.

tropical Pacific interannual variability. This is in contrast to our findings, where the deepening of the thermocline in SPac−2°C experiment is accompanied by increased ENSO variability, while in the SPac+2°C experiment a shoaling of the thermocline goes along with a weakening of ENSO. This inconsistency between the Cane–Zebiak-derived model used by Fedorov and Philander and our results may be explained by details of the thermocline change. In our experiments the thermocline change is small in the eastern Pacific, where it should have the biggest impact on ENSO variability through changes in the thermocline feedback. However, Fedorov and Philander (2001) results are based on a very simple model and may not be able to fully explain a complex GCM model.

c. *Feedback changes*

Changes in relevant positive/negative feedbacks generated by the change in the mean state will impact ENSO. We have estimated the strength of the atmosphere–ocean coupling using both scatterplots and regression analysis of Niño-3 SST anomalies against zonal wind stress, thermocline depth, and net surface heat flux anomalies. One cause for the decrease in ENSO variability in response to an enhanced warming in the subtropical South Pacific might be the reduction in central Pacific zonal wind stress sensitivity to eastern Pacific SST. We found that the atmospheric sensitivity is reduced by about 10% in the SPac+2°C experiment, while it has slightly increased in the case of the SPac−2°C experiment (not shown). The SST–thermocline feedback is increased (decreased) by about 1°C m^{-1} in the central-eastern Pacific for the SPac+2°C (SPac−2°C) experiment relative to the control integration (not shown) and is consistent with changes in the thermocline depth. For example, in the SPac+2°C experiment, the shallower equatorial thermocline will lead to an enhancement of the thermocline feedback, which in turn will increase ENSO variability, in contrast to our findings (Fig. 8a). We found no significant changes in the eastern SST net surface heat flux damping in both sensitivity experiments (not shown).

Although the changes in the atmospheric sensitivity contribute to the changes in ENSO variability, they cannot explain the magnitude of the variability changes observed in our sensitivity experiments. According to the linear framework (Fedorov and Philander 2001), a relatively shallow thermocline favors the high-frequency local modes (SST modes) in which SST changes depend on wind-induced upwelling and advection. Because our model has a rather shallow zonal mean thermocline (100 m), we suggest that the zonal temperature gradient changes are the main contributors to the modulation of ENSO variability in our South Pacific sensitivity experiments. Following An and Wang (2000), we compute the lag regression of $(-u'\overline{T}_x)$

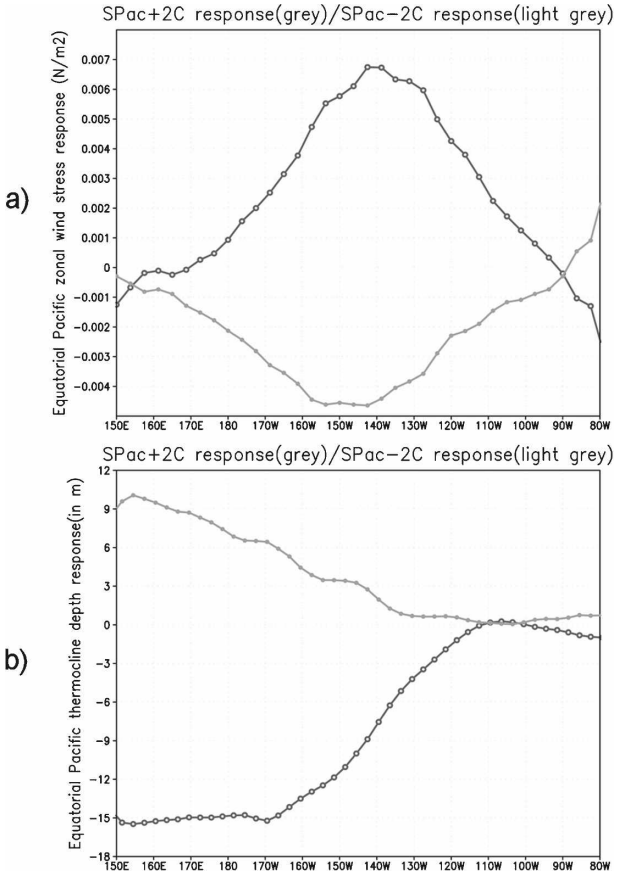

FIG. 12. (a) Anomalous zonal wind stress (N m^{-2}) in the SPac+2°C (gray curve with open circles), and the SPac−2°C experiments (light gray curve). (b) Anomalous depth of the thermocline (m) in the SPac+2°C (gray curve with open circles), and the SPac−2°C experiments (light gray curve). The anomalies are computed as the spatial average between 5°S and 5°N.

(the so-called zonal advective feedback) upon the Niño-3 SSTA index, as a function of longitude and phase lag, for the control run and SPac±2°C experiments. The SST tendency west of 150°W is nearly in phase with the Niño-3 SST anomaly for both the control run and the SPac−2°C (SPac+2°C) experiment, but is stronger (weaker) in the latter (not shown). The zonal advective feedback is in phase with SST variations over the eastern tropical Pacific and does not impact the ENSO frequency in our coupled model. Therefore, this increase (decrease) in the zonal advective feedback only leads to an intensification (weakening) of ENSO variability in our simulations.

d. Annual cycle changes and their effect on ENSO

Observational and modeling evidence exists indicating that the strength of ENSO may be anticorrelated with the strength of the annual cycle in the eastern equatorial Pacific (Gu and Philander 1995; Guilyardi 2006; Timmermann et al. 2007). Liu (2002) used a conceptual model to study the effect of an external periodic forcing on the amplitude and period of ENSO and found that nonlinear frequency entrainment enables the external forcing, such as the annual forcing, to damp ENSO significantly. For a weak annual cycle ENSO will maintain its eigenfrequency, while for a very strong annual cycle ENSO's frequency will be completely entrained into the forcing frequency and the interannual variability will be weakened. We shall first diagnose the changes in the equatorial annual cycle in our SPac±2°C experiments. Then, we shall investigate the impact of these changes on the ENSO statistics.

The monthly standard deviation and the annual cycle of the Niño-3 SSTA for the SPac±2°C experiments and the control integration are depicted in Fig. 13. Our results are consistent with the above-mentioned theory: in response to an enhanced warming in the subtropical South Pacific, the annual cycle in the equatorial Pacific intensifies and, therefore, helps to weaken ENSO. The opposite is valid for the SPac−2°C experiment: forced by a cold subtropical South Pacific, the equatorial annual cycle weakens and this contributes to the intensification of ENSO.

Furthermore, the remote subtropical forcing can also change ENSO frequency through changes in the strength of the annual cycle. Figure 10b suggests a shift to a longer ENSO period in the colder climate of SPac−2°C experiment. The main peak in the ENSO spectrum is located at 42 months as opposed to 37 months in the control simulation. This shift toward a longer period of ENSO in the SPac−2°C experiment may be partly attributed to the weakening of the annual cycle. In the warmer climate of the SPac+2°C experiment, the strengthening of the equatorial annual cycle may also explain the broadening of ENSO spectrum with increased energy in the high-frequency range (Fig. 10a).

5. Conclusions and discussion

In this study, connections between the tropical and subtropical Pacific on decadal time scales are investigated using specifically designed experiments performed with the state-of-art ocean–atmosphere–ice coupled model ECHAM5/MPI-OM. Because the available observational data are insufficient for these time scales, the research in this study focused on model analysis.

Comparing the warming and the cooling experiments in both the North and South Pacific we conclude that the subtropical South Pacific appears to "affect" more the equatorial ocean than the subtropical North Pacific.

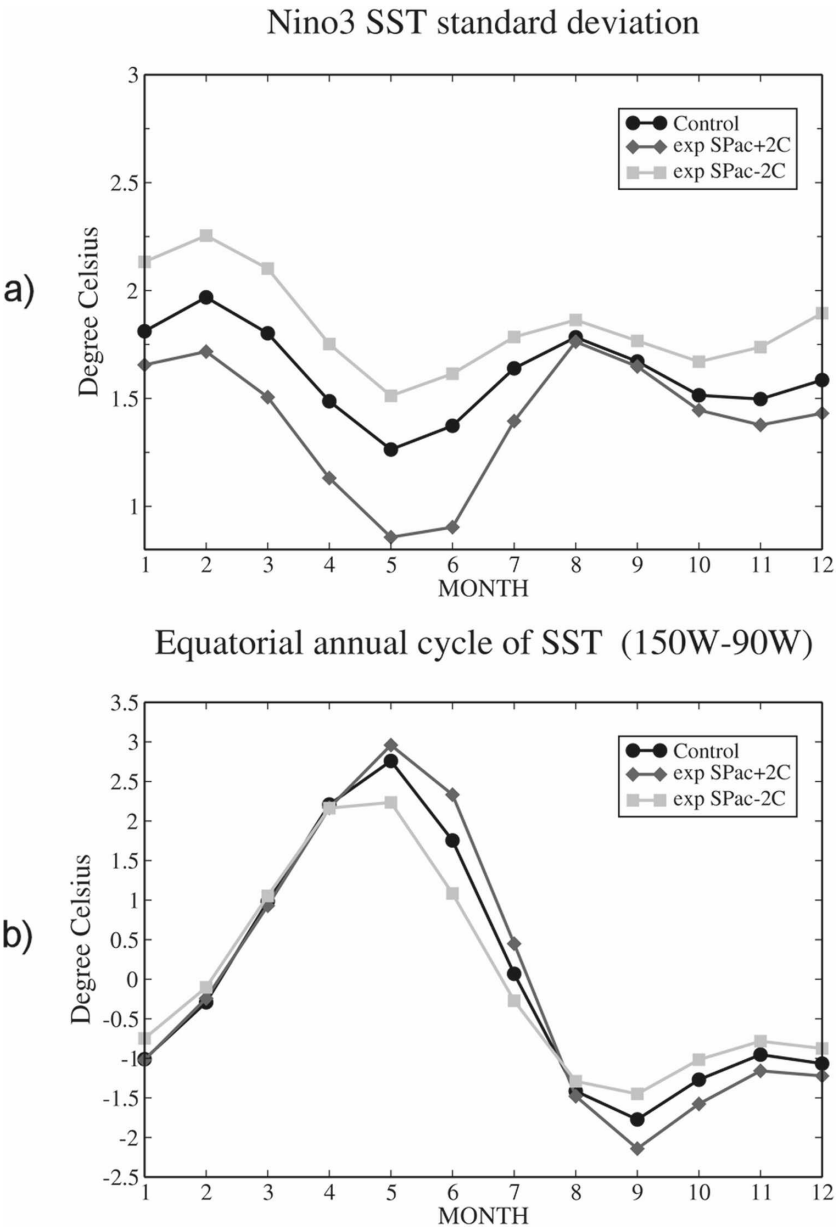

FIG. 13. (top) Monthly standard deviation of the Niño-3 SSTA (°C). (bottom) Annual cycle of the Niño-3 SSTA (°C). In both panels, the dark gray (light gray) curves are obtained from the SPac+2°C (SPac−2°C) experiment, while the black curves represent the control integration.

The larger contribution of the South Pacific is consistent with observational (Johnson and McPhaden 1999) and modeling studies using an OGCM (Yang et al. 2004) or fully coupled GCM (Yang et al. 2005a; Yang and Liu 2005). The partial coupling idealized experiments employed by Yang and Liu (2005) and Yang et al. (2005a) show that the impact of South Pacific extratropical thermal forcing (poleward of 30°S) on the tropical climate is 30%–50% larger than the impact of North Pacific extratropics. Note that Yang et al. (2005a) investigated only the effect of extratropical Northern and Southern Hemisphere warming on tropical Pacific climate and did not consider the impact of a cooling. In our sensitivity experiments, we found an asymmetric impact of the North and South Pacific Ocean on the tropical climate not only in the case of enhanced subtropical warming, but also for an enhanced subtropical cooling.

Our model results suggest that the subtropics affect equatorial surface climate mainly through atmosphere–mixed layer interactions for the South Pacific Ocean, and through the slow "oceanic tunnel" for the North Pacific Ocean. This explains the different time scale of the response in the two experiments. The weak effect of the atmosphere–mixed layer interactions in the North Pacific experiment might also be attributed to a weak atmospheric response to the thermal forcing in the subtropical North Pacific, as indicated by the results of our atmosphere-only sensitivity experiments.

The remote subtropical climate variations can also modulate the behavior of ENSO through changes in the background mean state of the tropical Pacific. We have shown that ENSO statistics exhibit significant changes both in amplitude and in frequency in response to the South Pacific subtropical thermal forcing. The simulated changes in the equatorial zonal thermal contrast are the main contributor to the modulation of ENSO variability. An enhanced warming (cooling) in the subtropical South Pacific is accompanied by a reduction (increase) in the equatorial zonal SST contrast that favors a weakening (intensification) of ENSO. The remote thermal forcing in the subtropical South Pacific can also alter the strength of the equatorial Pacific annual cycle and, thus, may partly explain the simulated shift in ENSO frequency. We have also investigated other alternative explanations for the simulated change in ENSO frequency, such as changes in ENSO structure (An and Wang 2000; An and Jin 2000) or in the propagation speed of Rossby/Kelvin waves, but none of these provided a satisfactory explanation. Because there are many processes that can affect ENSO frequency, and because this model has a rather coarse resolution, it is difficult for us to pinpoint the cause for changes in ENSO frequency.

This study suggests that subtropical South Pacific climate variations play a dominant role in tropical Pacific decadal variability and in the decadal modulation of ENSO activity. However, our results may be limited by model biases typical of many non-flux-corrected coupled models. Therefore, they need to be tested in other state-of-the-art coupled GCMs. We also need to be cautious about the interpretation of the initial atmospheric responses, because the discussions here are based on a single integration, which may be contaminated by the internal variability of the coupled model. Ensemble integrations represent a better experimental approach.

Acknowledgments. The authors thank Monika Esch for help with the ECHAM5 model, Dr. Jürgen Bader and Dr. Eric Guilyardi for helpful discussions, and Dr. Wolfgang Mueller for valuable comments on an earlier version of the manuscript. This work was supported by the International Max Planck Research School on Earth System Modelling and the Zeit Foundation Ebelin and Gerd Bucerius. We also acknowledge the support of European Union's Framework Programme VI via the DYNAMITE project (Contract 003903). The numerical model integrations were performed at the DKRZ (Deutsches Klimarechenzentrum) in Hamburg, Germany. We also thank the two anonymous reviewers for their very constructive comments and suggestions.

REFERENCES

An, S.-I., and F.-F. Jin, 2000: An eigen analysis of the interdecadal changes in the structure and frequency of ENSO mode. *Geophys. Res. Lett.,* **27,** 2573–2576.

——, and B. Wang, 2000: Interdecadal change of the structure of ENSO mode and its impact on the ENSO frequency. *J. Climate,* **13,** 2044–2055.

Barnett, T., D. W. Pierce, M. Latif, D. Dommenget, and R. Saravana, 1999: Interdecadal interactions between the tropics and the midlatitudes in the Pacific basin. *Geophys. Res. Lett.,* **26,** 615–618.

Collins, M., and CMIP Modeling Groups, 2005: El Niño or La Niña-like climate change? *Climate Dyn.,* **24,** 89–104.

D'Arrigo, R., E. R. Cook, R. J. Wilson, R. Allan, and M. E. Mann, 2005: On the variability of ENSO over the past six centuries. *Geophys. Res. Lett.,* **32,** L03711, doi:10.1029/2004GL022055.

Deser, C., M. A. Alexander, and M. S. Timlin, 1996: Upper-ocean thermal variations in the North Pacific during 1970-1991. *J. Climate,* **9,** 1840–1855.

——, A. S. Phillips, and J. W. Hurrel, 2004: Pacific interdecadal climate variability: Linkage between the Tropics and the North Pacific during boreal winter since 1900. *J. Climate,* **17,** 3109–3124.

Fedorov, A. V., and S. G. Philander, 2001: A stability analysis of tropical ocean–atmosphere interaction: Bridging measurements and theory for El Niño. *J. Climate,* **14,** 3086–3101.

Giese, B. S., S. C. Urizar, and N. S. Fučkar, 2002: Southern Hemisphere origins of the 1976 climate shift. *Geophys. Res. Lett.,* **29,** 1014, doi:10.1029/2001GL013268.

Gu, D., and S. G. H. Philander, 1995: Secular changes of annual and interannual variability in the tropics during the past century. *J. Climate,* **8,** 864–876.

——, and ——, 1997: Interdecadal climate fluctuations that depend on exchange between the Tropics and extratropics. *Science,* **275,** 805–807.

Guilyardi, E., 2006: El Niño-mean state–seasonal cycle interactions in a multi-model ensemble. *Climate Dyn.,* **26,** 329–348.

Holland, C. L., R. Scott, S.-I. An, and F. W. Taylor, 2006: Propagating decadal sea surface temperature signal identified in the modern proxy records of the tropical Pacific. *Climate Dyn.,* **28,** 163–179, doi:10.1007/s00382-006-0174-0.

Huang, B., and Z. Liu, 1999: Pacific subtropical-tropical thermocline exchange in the National Centers for Environmental Prediction ocean model. *J. Geophys. Res.,* **104,** 11 065–11 076.

Johnson, G. C., and M. J. McPhaden, 1999: Interior pycnocline flow from the subtropical to equatorial Pacific Ocean. *J. Phys. Oceanogr.,* **29,** 3073–3089.

Jungclaus, J. H., and Coauthors, 2006: Ocean circulation and tropical variability in the coupled Model ECHAM5/MPI-OM. *J. Climate,* **19,** 3952–3972.

Kerr, R. A., 2004: Three degrees of consensus. *Science,* **305,** 932–934.

Kleeman, R., J. P. McCreary, and B. A. Klinger, 1999: A mechanism for generating ENSO decadal variability. *Geophys. Res. Lett.,* **26,** 1743–1746.

Knutson, T. R., S. Manabe, and D. Gu, 1997: Simulated ENSO in a global coupled ocean model: Multidecadal amplitude modulation and CO_2 sensitivity. *J. Climate,* **10,** 138–161.

Latif, M., and T. P. Barnett, 1994: Causes of decadal climate variability over the North Pacific and North America. *Science,* **266,** 634–637.

——, and Coauthors, 2001: ENSIP: The El Niño Simulation Intercomparison Project. *Climate Dyn.,* **18,** 255–276.

Lea, D. W., 2004: The 100 000-year cycle in tropical SST, greenhouse forcing, and climate sensitivity. *J. Climate,* **17,** 2170–2179.

Liu, Z., 1996: Modelling the equatorial annual cycle with a linear coupled model. *J. Climate,* **9,** 2376–2385.

——, 2002: A simple model study of the forced response of ENSO to an external periodic forcing. *J. Climate,* **15,** 1088–1098.

——, and S. P. Xie, 1994: Equatorward propagation of coupled air–sea disturbances with application to the annual cycle of the eastern tropical Pacific. *J. Atmos. Sci.,* **51,** 3807–3822.

——, and H. Yang, 2003: Extratropical control of tropical climate, the atmospheric bridge and oceanic tunnel. *Geophys. Res. Lett.,* **30,** 1230, doi:10.1029/2002GL016492.

——, S. G. H. Philander, and R. Pacanowski, 1994: A GCM study of tropical-subtropical upper ocean mass exchange. *J. Phys. Oceanogr.,* **24,** 2606–2623.

——, S. Vavrus, F. He, N. Wen, and Y. Zhong, 2005: Rethinking tropical ocean response to global warming: The enhanced equatorial warming. *J. Climate,* **18,** 4684–4700.

Lohmann, K., and M. Latif, 2005: Tropical Pacific decadal variablity and the subtropical cells. *J. Climate,* **18,** 5163–5178.

Luo, J.-J., and T. Yamagata, 2001: Long-term El Niño-Southern Oscillation (ENSO)-like variations with special emphasis on the South Pacific. *J. Geophys. Res.,* **106,** 22 211–22 227.

——, S. Mason, S. Behera, P. Delecluse, S. Gualdi, A. Novarra, and T. Yamagata, 2003: South Pacific origin of the decadal ENSO-like variation as simulated by a coupled GCM. *Geophys. Res. Lett.,* **30,** 2250, doi:10.1029/2003GL018649.

Luo, Y., L. Rothstein, R.-H. Zhang, and A. Busalacchi, 2005: On the connection between South Pacific subtropical spiciness anomalies and decadal equatorial variability in an ocean general circulation model. *J. Geophys. Res.,* **110,** C10002, doi:10.1029/2004JC002655.

Marsland, S., H. Haak, J. Jungclaus, M. Latif, and F. Röske, 2003: The Max-Planck-Institute global ocean/sea ice model with orthogonal curvilinear coordinates. *Ocean Modell.,* **5,** 91–127.

Merryfield, W. J., 2006: Changes in ENSO under CO_2 doubling in the IPCC AR4 coupled climate models. *J. Climate,* **19,** 4009–4027.

McCreary, J., and P. Lu, 1994: Interactions between the subtropical and equatorial ocean circulations: The subtropical cell. *J. Phys. Oceanogr.,* **24,** 466–497.

McPhaden, M., and D. Zhang, 2002: Slowdown of the meridional overturning circulation in the upper Pacific Ocean. *Nature,* **415,** 603–608.

——, and ——, 2004: Pacific Ocean circulation rebounds. *Geophys. Res. Lett.,* **31,** L18301, doi:10.1029/2004GL020727.

Meehl, G. A., H. Teng, and G. Branstator, 2006b: Future changes of El Niño in two global coupled models. *Climate Dyn.,* **26,** 581–609.

Miller, A. J., and N. Schneider, 2000: Interdecadal climate regime dynamics in the North Pacific Ocean: Theories, observation and ecosystem impacts. *Prog. Oceanogr.,* **47,** 355–379.

Nitta, T., and S. Yamada, 1989: Recent warming of tropical sea surface temperature and its relationship to the Northern Hemisphere Circulation. *J. Meteor. Soc. Japan,* **67,** 375–383.

Nonaka, M., and S.-P. Xie, 2000: Propagation of North Pacific interdecadal subsurface temperature anomalies in an ocean GCM. *Geophys. Res. Lett.,* **27,** 3747–3750.

——, ——, and J. McCreary, 2002: Decadal variations in the subtropical cells and equatorial Pacific SST. *Geophys. Res. Lett.,* **29,** 1116, doi:10.1029/2001GL013717.

Pierce, D. W., T. P. Barnett, and M. Latif, 2000: Connections between the Pacific Ocean Tropics and midlatitudes on decadal timescales. *J. Climate,* **13,** 1173–1194.

Roeckner, E., and Coauthors, 2003: The atmosphere general circulation model ECHAM5, Part 1: Model description. Max-Planck-Institute für Meteorologie Rep. 349, 127 pp.

——, and Coauthors, 2006: Sensitivity of simulated climate to horizontal and vertical resolution in the ECHAM5 atmosphere model. *J. Climate,* **19,** 3771–3791.

Schneider, N., A. J. Miller, M. A. Alexander, and C. Deser, 1999a: Subduction of decadal North Pacific temperature anomalies: Observations and dynamics. *J. Phys. Oceanogr.,* **29,** 1056–1070.

——, S. Venzke, A. J. Miller, D. W. Pierce, T. P. Barnett, C. Deser, and M. Latif, 1999b: Pacific thermocline bridge revisited. *Geophys. Res. Lett.,* **26,** 1329–1332.

Sun, D.-Z., T. Zhang, and S.-I. Shin, 2004: The effect of subtropical cooling on the amplitude of ENSO: A numerical study. *J. Climate,* **17,** 3786–3798.

Timmermann, A., and Coauthors, 2007: The influence of a weakening of the Atlantic meridional overturning circulation on ENSO. *J. Climate,* **20,** 4899–4919.

Trenberth, K. E., and J. W. Hurrell, 1994: Decadal atmosphere-ocean variations in the Pacific. *Climate Dyn.,* **9,** 303–319.

Van Oldenborgh, G. J., S. Y. Philip, and M. Collins, 2005: El Niño in a changing climate: A multi-model study. *Ocean Sci.,* **1,** 81–95.

Vimont, D., J. M. Wallace, and D. S. Battisti, 2001: Footprinting: A seasonal connection between the midlatitudes and tropics. *Geophys. Res. Lett.,* **28,** 3923–3927.

Wang, D. X., and Z. Liu, 2000: The pathway of interdecadal variability in the Pacific Ocean. *Chinese Sci. Bull.,* **45,** 1555–1561.

Wu, L., Z. Liu, C. Li, and Y. Sun, 2006: Extratropical control of recent tropical Pacific decadal climate variability: A relay teleconnection. *Climate Dyn.,* **28,** 99–112, doi:10.1007/s00382-006-0198-5.

Xie, S.-P., and S. G. H. Philander, 1994: A coupled ocean-atmosphere model of relevance to the ITCZ in the eastern Pacific. *Tellus,* **46A,** 340–350.

Yang, H., and Z. Liu, 2005: Tropical-extratropical climate interaction as revealed in idealized coupled climate model experiments. *Climate Dyn.,* **24,** 863–879, doi:10.1007/s00382-005-0021-8.

——, ——, and H. Wang, 2004: Influence of extratropical thermal and wind forcing on equatorial thermocline in an ocean GCM. *J. Phys. Oceanogr.,* **34,** 174–187.

——, H. Jiang, and B. Tan, 2005a: Asymmetric impact of the North and South Pacific on the equator in a coupled climate model. *Geophys. Res. Lett.,* **32,** L05604, doi:10.1029/2004GL022195.

——, Q. Zhang, Y. Zhong, S. Vavrus, and Z. Liu, 2005b: How does extratropical warming affects ENSO? *Geophys. Res. Lett.,* **32,** L01702, doi:10.1029/2004GL021624.

Zelle, H., G. J. van Oldenborgh, G. Burgers, and H. A. Dijkstra, 2005: El Niño and greenhouse warming: Results from ensemble simulations with the NCAR CCSM. *J. Climate,* **18,** 4669–4683.

Zhang, R.-H., T. Kagimoto, and S. Zebiak, 2001: Subduction of decadal North Pacific thermal anomalies in an ocean GCM. *Geophys. Res. Lett.,* **28,** 2449–2452.

Zhang, Y., J. M. Wallace, and D. S. Battisti, 1997: ENSO-like interdecadal variability: 1900–93. *J. Climate,* **10,** 1004–1020.